Chemical Engineering Journal 425 (2021) 130424

Contents lists available at ScienceDirect

Chemical Engineering Journal

journal homepage: www.elsevier.com/locate/cej

Performance comparison between washcoated and packed-bed monolithic reactors for the low-temperature Fischer-Tropsch synthesis

María Ibáñez [a], Oihane Sanz [a,*], Ane Egaña [a], Inés Reyero [b], Fernando Bimbela [b], Luis M. Gandía [b], Mario Montes [a]

[a] Applied Chemistry Department, Chemistry Faculty, University of the Basque Country (UPV/EHU), Donostia-San Sebastián, Spain
[b] Grupo de Reactores Químicos y Procesos para la Valorización de Recursos Renovables, Sciences Department and Institute for Advanced Materials and Mathematics (InaMat^2), Universidad Pública de Navarra, 31006 Pamplona, Spain

ARTICLE INFO

Keywords:
Fischer-Tropsch synthesis
Coated monolith
Packed-bed monolith
C5+ productivity
Characteristic diffusion length

ABSTRACT

Washcoating and packing of Co-Re catalyst particles have been employed as structuring methods of parallel channel monoliths used in the low-temperature Fischer-Tropsch synthesis (FTS). These methods were compared with regard to catalyst hold-up, heat transfer properties and pressure drop. Reactors output was assessed in terms of CO conversion, CH_4 selectivity and productivity of C5+ hydrocarbons. Washcoating led to much lower pressure drops, but also resulted in considerably lower catalyst inventory. As for the reactors performance (volumetric and per catalyst mass C5+ productivities), the washcoated monoliths were more effective than the packed-bed ones. This has been attributed to their more favorable hydrodynamic behavior that facilitates the drainage of the reaction products (liquids and waxes) through the central hollow of the channels thus reducing the extra-pellet diffusional limitations. For both catalyst configurations, it has been found that the productivity of C5+ per catalyst mass unit increases as the characteristic diffusion length increases within the range of values considered in this study (below 150 μm). This indicates that a moderate level of internal mass transport restrictions is beneficial for the low-temperature FTS, which has been explained in terms of the effects of diffusional limitations on the H_2/CO molar ratio, and that of this ratio on the FTS kinetics. The possible influence of thermal effects on these results has been numerically and experimentally discarded.

1. Introduction

Over the last few years, a major concern has arisen regarding the decreasing global oil reserves, driven by a strong world energy demand and by political instabilities in oil producing regions. Thus, there is nowadays a strong need for alternative sources to meet the world demand for liquid fuels [1]. Within this context, the low-temperature Fischer-Tropsch Synthesis (FTS) is one of the most reliable routes to produce liquid hydrocarbons from nonpetroleum resources.

The FTS is a multiphase heterogeneously catalyzed reaction that allows converting synthesis gas, a mixture of CO and H_2, primarily into liquid hydrocarbons and solid waxes [2]. Historically, syngas was first produced from coal by gasification (coal-to-liquid or CTL process), and more recently, mainly by the steam reforming or partial oxidation of natural gas (gas-to-liquid or GTL process) [2,3]. In the last years, the gasification of biomass (BTL process) or organic wastes (WTL process) have been proposed as sustainable FTS routes [1].

The synthetic hydrocarbons obtained (high-purity alkanes and olefins as well as oxygenates) can be used as feedstock for the chemical industry, or for the production of synthetic fuels such as gasoline, diesel, and kerosene. The process yields clean fuels free from sulfur that have been proven to produce less soot during combustion [2,4].

The synthesis reaction equations can be written as follows [2]:

$$nCO + (2n+1)H_2 \rightarrow C_nH_{2n+2} + nH_2O \quad (1)$$

$$nCO + 2nH_2 \rightarrow C_nH_{2n} + nH_2O \quad (2)$$

$$nCO + 2nH_2 \rightarrow C_nH_{2n+2}O + (n\text{-}1)H_2O \quad (3)$$

$$CO + 3H_2 \rightarrow CH_4 + H_2O \quad (4)$$

$$CO + H_2O \leftrightarrow CO_2 + H_2 \quad (5)$$

$$2CO \rightarrow C + CO_2 \quad (6)$$

* Corresponding author.
E-mail address: oihane.sanz@ehu.eus (O. Sanz).

https://doi.org/10.1016/j.cej.2021.130424
Received 14 January 2021; Received in revised form 12 May 2021; Accepted 15 May 2021
Available online 2 June 2021

Obviously, CH_4 and CO_2 are undesirable products in the FTS. The so-called low-temperature FTS is carried out over supported cobalt-based catalyst at 20–40 bar and temperatures below 240 °C [5–8]. The FTS is a highly exothermic reaction (ΔH°_R = -165 kJ/mol), thus reaction heat removal becomes a big challenge for commercial units. The efficient removal of heat is key because the products distribution is strongly dependent on the reaction temperature. In this regard, an inefficient temperature control leading to relatively high temperatures would shift the products distribution toward lighter hydrocarbons, mainly methane [9–11]. Achieving fast heat transfer is one of the main problems for conducting FTS in fixed-bed reactors (FBRs) [12]. Metallic monolithic substrates with high thermal conductivity are a real alternative to traditional FBRs, showing greatly improved heat transfer capabilities in FTS [6,9,12]. These structured catalysts also allow nearly isothermal operation when conducting reactions with high thermal effects; furthermore, intraparticle transport limitations are alleviated and pressure drop is greatly reduced [13].

The method most frequently used to prepare monolithic catalysts for FTS is washcoating [9,10,14–19]. In this method, the monolithic substrate is immersed in a slurry of the catalyst at controlled speed for a short period of time; then, the substrate is removed and most liquid is shaken out. Finally, the coating is fixed to the substrate walls by calcination at suitable temperature. The preparation of the catalyst slurry is a key stage of this manufacturing process. In addition to a suitable formulation to obtain adherent and homogeneous catalyst layers, it is necessary that the coating process does not impair the activity, selectivity and stability of the catalyst. The slurry preparation requires the optimization and control of a number of relevant physicochemical variables which are specific of every catalytic material [20,21]: the catalyst particle characteristics (particle size distribution, zeta potential, etc.), the solids content, the nature and concentration of additives (binders, surfactants, etc.), and the dispersion medium (water, alcohols, etc.)

Sometimes, the used additives and/or the thermal treatments performed modify the activity of the catalyst when the ready-made catalyst slurry is prepared [22]. We have developed an "All-in-One" washcoating procedure according to which an aqueous slurry containing all the required components, namely the catalytic support, precursors of the active phases, and additives is prepared in a single step [14,22]. This method is suitable to washcoat a variety of substrates such as monoliths, foams and microchannel reactors made of different materials [9,14,23]. In addition, drying and calcination of that slurry leads to a powder catalyst, the so-called slurried catalyst, with the same composition and preparation and thermal histories than the one deposited onto the monoliths. This is very useful to conduct characterization analyses and catalytic performance assessment tests as it is possible to obtain a catalyst with similar physicochemical properties to the one present in the structured systems [9,23].

Usually, the catalyst layer deposited on monoliths for FTS is very thin, motivated by the negative effects of internal heat and mass transport limitations on the reaction selectivities to the desired long-chain hydrocarbons. It has been observed that ceramic monoliths coated with layers thicker than 50 μm suffer from significant transport limitations, leading to poor C5+ selectivity and increased methane production [15,17,18]. In contrast, using a highly conductive aluminum monolith it is possible to work with catalyst layer thicknesses of up to 90 μm without significant loss of hydrocarbon selectivity [9], thus evidencing the influence of the FTS thermal effect on the reaction selectivity. Therefore, a highly effective thermal conductivity of the substrates is convenient for an adequate temperature control of FTS in structured catalysts.

It should be noted that conventional Co-based catalysts for low-temperature FTS exhibit low specific activity. Therefore, it is important to maximize the catalyst inventory in the reactor for being able of achieving high productivities per reactor volume unit. It is well known that the catalyst inventory on coated monoliths may be insufficient because the geometric surface area of commercially available structured reactors is too small (typically below 4 m^2/g [24]). This fact points to the requirement of substrates with very high cell densities in case of considering this type of structured catalysts at the industrial scale [6]. We have recently demonstrated that high-cell-density monoliths (2250 cpsi) with large geometric surface area (88 cm^2/cm^3) can be made by corrugation of thin aluminum foils, allowing to achieve high catalyst hold-ups (up to 0.33 g/cm^3) with layer thicknesses thinner than 50 μm [9,17].

To increase the catalyst load of monolithic reactors, the use of "structured packed-beds" has been recently proposed for FTS [25,26,27]. Monoliths are favorable geometries for catalyst hosting by immobilization in the form of catalyst particles randomly packed in the channels [28,29]. This configuration improves the heat transfer properties of conventional FBRs, overcomes the complications associated to the washcoating process and greatly increases the catalyst inventory compared to a coated structured reactor. In this regard, the catalyst volumetric load can be doubled (0.6 g/cm^3) in a 270 cpsi aluminum monolith (0.94 void fraction) filled with catalyst particles of 300 μm [27].

In the case of structured packed-beds, the larger channel wall area relative to the reactor volume leads to higher bed porosity compared to conventional packed beds thus allowing the use of smaller and more effective catalyst particles [29]. In this regard, Fratalochi *et al.* [30] stated that catalyst particles with diameters of 400–800 μm can be used while granting acceptable pressure drops.

In the present work, several washcoated and packed-bed monolithic reactors made of corrugated aluminum foils are compared as concerns catalyst hold-up and C5+ volumetric production. In all cases, the same Co-Re/Al_2O_3 catalyst prepared using the "All-in-One" method was used in the FTS. As for washcoated reactors, aluminum monoliths with different cell densities were coated to obtain a wide range of catalyst layer thicknesses though keeping constant the catalyst load. In the case of the packed-bed monoliths, different catalyst particle sizes have been used. All reactors were tested in the FTS under similar operation conditions.

2. Experimental

2.1. Monoliths preparation

Parallel channels monoliths with four different cell densities, denoted R1 to R4 (see Table 1) were prepared using high-purity aluminum foils supplied by INASA (above 99% (w/w) Al content and thickness of 82 μm). Monoliths were prepared by rolling alternating flat and corrugated sheets into cylinders of 16 mm diameter and 30 mm length, achieving a total monolith volume of 6.03 cm^3. The aluminum monoliths were pretreated to produce surface roughness in order to promote catalyst coating adherence. To this end, the monoliths were introduced in an alkaline medium (pH of 10.5) for several minutes, dried, and finally calcined in air at 500 °C for 2 h [9]. The geometric characteristics of the different monoliths prepared are summarized in Table 1.

2.2. Monolithic catalyst preparation

The washcoated monoliths were prepared using the so-called 'All-in-

Table 1
Geometric parameters of the metallic monoliths employed.

Monolith type	Cell density (cpsi)	Geometric surface area (cm^2/monolith)	Void fraction	Hydraulic diameter, D_H (μm)	$k_{e,r}$(W/m·K)[1]
R1	2360	375	0.75	347	34.3
R2	1330	338	0.78	475	29.6
R3	465	219	0.85	827	16.8
R4	289	162	0.89	1132	12.9

[1] Radial effective thermal conductivity calculated according to ref.[31]

One' washcoating procedure [9]. An aqueous suspension was prepared, containing the cobalt precursor, $Co(NO_3)_3{\cdot}6H_2O$ (Sigma-Aldrich), the precursor of the Re promoter, Re_2O_7 (Alfa Aesar), and the support, γ-Al_2O_3 (Spheralite, Procatalyse SCS505), previously grounded for 5 min in a disks mill and then for 30 min in a ball mill. The suspension formulation included a small quantity of a commercial colloidal alumina suspension (Nyacol® Al20) used as binder. The nominal catalyst composition was 20 wt% Co–0.5 wt% Re/Al_2O_3 [9].

As for the packed-bed monoliths preparation, the slurried catalyst was employed. This is the powder catalyst obtained by drying and calcination of the suspension used for preparing washcoated monoliths. The catalyst was ground and sieved to get fractions of different particle sizes within 150–900 μm. All packed-bed reactors were prepared using monolith type R4; this monolith presents the highest void fraction (Table 1), thus allowing the packing of the highest amount of catalyst. The monolith was first inserted into a FeCrAl alloy cylindrical cartridge, and secured with a FeCrAl alloy mesh welded on the cartridge bottom and glass wool. After that, the monolith channels were filled with slurried catalyst particles.

Monolithic catalysts were referred to as A_BC, where A is the type of monolith used (R1, R2, R3 or R4), B is the type of structuring method employed (W for washcoating and P for packing) and C is the nominal catalyst coating thickness (W method) or catalyst mean particle diameter (P method).

2.3. Catalysts characterization

The adherence of the catalyst layer deposited onto structured substrates was assessed by measuring the weight loss caused by exposure to ultrasound [32]. Washcoated monoliths were immersed in vials filled with petroleum ether and sonicated for 30 min. Then, the excess liquid was removed by air blowing, drying at 100 °C for 1 h, and soft calcination in air at 200 °C for 2 h. Adherence is expressed as the percentage of the catalyst load that remained after ultrasonication.

Textural properties were assessed by N_2 adsorption–desorption (Micromeritics ASAP 2020). The experimental procedure for determining physical properties consisted of degasifying the samples (slurried catalyst and washcoated monoliths) at 180 °C and 10^{-3} mm Hg for 8 h to remove possible impurities, followed by N_2 adsorption–desorption in multiple equilibrium steps until sample saturation was achieved at −196 °C. Brunauer-Emmett-Teller (BET) and Barrett-Joyner-Halenda (BJH) formalisms were applied to the data of the desorption isotherm branch to obtain the specific surface area and the pore size distribution, respectively.

Dynamic pulse CO chemisorption was also performed for coated structured and slurried catalysts by an AutoChemII 2920 station from Micromeritics. Samples placed in a U-shaped quartz holder (12 mm i.d. for the powdered catalyst and 22 mm i.d. for coated structured substrates) were pretreated under H_2 at 350 °C for 10 h. Then, catalysts were cooled to a chemisorption temperature of 100 °C. The volume of the injection loop was 0.5 cm^3. Pulses of CO were injected using H_2 as carrier gas [23]. The CO chemisorption was measured by difference with the peak area of the pulses upon surface saturation recorded by a thermal conductivity detector after calibration.

The temperature-programmed reduction (TPR) measurements were carried out in a Micromeritics Autochem II 2920 apparatus equipped with a TCD detector. Typically, about 60 mg of the catalyst were placed on a U-shaped quartz tube upon a quartz wool bed. H_2 consumed profiles were recorded by monitoring the TCD signal from − 20 °C to 1000 °C at a heating rate of 10 °C/min in a 50 cm^3/min flowing 10% H_2-Ar mixture.

X-ray Diffraction (XRD) patterns of the slurried catalysts were recorded using a Bruker D8 Advance Diffractometer with CuKα radiation ($\lambda = 0.154$ nm) and a graphite monochromator, operating at 40 kV and 30 mA. Samples were scanned within a 2θ range of 5–85° in steps of 0.05° per 5-s pass.

Pressure drops caused by gas flow through the coated and packed structured substrates at different velocities were measured with a Digitron 2080P Pressure Meter. Volumetric air flows between 0.04 and 0.48 NL/min were used.

2.4. Catalytic tests and product analysis

FTS catalytic tests of structured reactors were carried out in a tubular Hastelloy reactor (17 mm i.d. for the monolithic catalysts and 8 mm i.d. for the powder catalyst). The tubular reactor was placed inside a commercial microreaction system from PID Eng&Tech. Three 1.5 mm o.d. thermocouples were used to measure the radial temperature profiles inside the monolithic catalysts. The thermocouples were placed at positions r = 0, r = R/2, and r = R, where r is the radial position, and R is the monolith radius (7.3 mm) (Fig. 1). Moreover, the axial temperature was also measured at two different positions using the thermocouple located at r = 0, namely at position l = 0 and l = L/2, where l is the axial position and L in the monolith length (30 mm) (Fig. 1). Radial (ΔT_R) and axial (ΔT_A) temperature differences were determined (Fig. 1). ΔT_R is the difference between the readings of the thermocouple located at the monolith center and that on the outer edge of the monolith at the same reactor length. ΔT_A is measured between the reaction temperature control point, located at the exit of the monolith at r = 0, and the measurement point located at the monolith center.

FTS catalytic tests on conventional packed beds were carried out in a tubular Hastelloy reactor of 8 mm i.d. The 450 mg of powder catalyst was diluted with 2.25 g of SiC. The control point of reaction temperature was located at the exit of the bed.

Reaction conditions were as follows: absolute total pressure, 20 bar; temperature, 220 °C; syngas space velocity of 3 LN $g_{cat.}^{-1}h^{-1}$, 96 h time-on-stream (TOS), and syngas feed H_2/CO molar ratio of 2. Prior to the FTS tests, the catalysts were reduced *in situ* at 350 °C with a pure H_2 stream flowing at 54 NmL/min for 10 h, to ensure that high degrees of cobalt reduction are achieved [33]. Then, the catalysts were cooled to 180 °C in H_2 flow and purged for 10 min with N_2. Finally, the syngas stream was fed, and the reactor was heated to 220 °C at 1 °C/min. A molar H_2/CO ratio of 2 was employed as feeding gas and 10 vol% of N_2 was used as internal standard to perform the gas chromatography (GC) analyses.

Gaseous products were analyzed online with an Agilent 6890 N GC equipped with three analysis lines. The first line was used to analyze

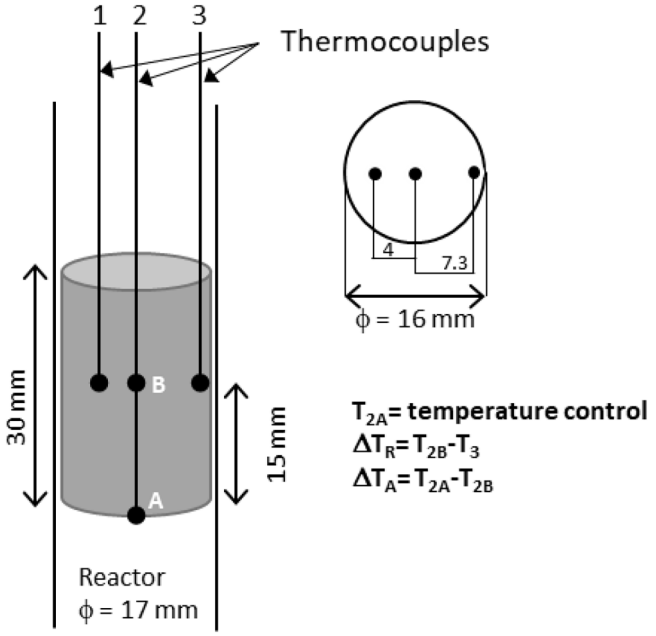

Fig. 1. Scheme of monolithic reactor with thermocouple positions.

light hydrocarbons (9 Foot Hayesep Q 80/100) and permanent gases (N_2, CO and H_2) (10-foot Molecular Sieve 13X 45/60). The second line was used to quantify hydrogen (10-foot Molecular Sieve 13X 45/60), and the third line was used to quantify hydrocarbons (60 m × 0.25 mm × 1.0 μm DB-1 capillary column). The first and second lines were connected to a TCD detector while the third one was connected to a FID detector.

CO conversion and products selectivity (%) were calculated using Eqs. (7) and (8), respectively. All the calculations were done on carbon basis.

$$CO\ conversion(\%) = \frac{(moles\ of\ CO)_{in} - (moles\ of\ CO)_{out}}{(moles\ of\ CO)_{in}} \times 100 \quad (7)$$

$$Selectivity\ of\ product\ C_i\ (\%) = \frac{(moles\ of\ carbon\ in\ product\ C_i)}{(moles\ of\ carbon\ in\ CO\ reacted)} \times 100 \quad (8)$$

3. Results

3.1. Catalyst hold-up

The nominal catalyst loading for washcoated monoliths was approximately 2000 mg (the maximum loading achieved without plugging the channels, Fig. 2), resulting in average catalyst layer thicknesses between 36 and 83 μm depending on the cell density (Table 2). The higher is the cell density of the monolith, the lower coatings are needed, due to the increase of the geometric surface area with cell density (Table 2). However, the resulting average catalyst hold-up, defined as the ratio of the catalyst mass to the volume occupied by the monolith, was 0.33 $g_{cat.}/cm^3$ for all washcoated monoliths. As for the layers adherence, all samples presented excellent adherence values, above 99%.

The packed-bed monoliths were prepared using the monolith (R4) having the highest void fraction (Fig. 2). Packing with particles of different sizes (from 150 to 950 μm) allowed to prepare monoliths with different catalyst hold-ups between 0.41 and 0.82 $g_{cat.}/cm^3$ (Table 2). Therefore, the catalyst inventory in all packed-bed monoliths is higher than in the coated monoliths.

In the framework of the present work, it is also important to consider the characteristic diffusion length (L_D) of a porous medium, which is defined as its volume divided by the area available for diffusion [34]. For spherical porous particles, the diffusion length equals one-sixth of their diameter ($D_{Particle}/6$). However, for a catalyst layer washcoated on a substrate, L_D directly corresponds to the layer thickness (δ). Consequently, the prepared monolithic catalyst presented different diffusion lengths. As can be seen in Table 2, the washcoated monoliths present values of L_D intermediate to those of the packed-bed monoliths.

3.2. Structured catalysts characterization

Before studying the results provided by the packed-bed and washcoated reactors in the FTS, it is necessary to check that the main physicochemical properties of the catalysts are similar for both types of structured systems. As for the textural properties, it can be seen in Table 3 that high specific surface areas around 175 m^2/g were obtained, which resulted somewhat more homogenous in the case of the packed-beds than for the washcoated catalysts. Mean specific pore volume of 0.25 cm^3/g and pore diameter of 5.4 nm were also obtained, showing no significant differences among the several structured catalysts. It is also remarkable the very similar cobalt dispersion of the different catalysts, that was around 7.5%. This is a very relevant result because it facilitates the comparison of the different catalytic systems, as cobalt dispersion effects can be discarded. The very similar metallic dispersions obtained are likely due to the use of the slurried powder catalyst to obtain the particles employed to prepare the packed-bed monoliths.

As concerns pressure drop (Fig. 3), the values are in general low, though they are between one to three orders of magnitude higher for the packed-bed reactors compared to the washcoated ones. This is an obvious effect of the important restriction to flow caused by the bed of catalyst particles. Indeed, for a given cell density (monolith R4), the pressure drop also increases as the catalyst particle sizes decreases (from reactors R4_P950 to R4_P150). As for the washcoated monolithic reactors, pressure drop values are extremely low under typical operating conditions, below 10^{-3} bar/m. In this case, apart from gas velocity, pressure drop is governed by the monolith cell density. In this regard, pressure drop increases as the cell density increases (from R4 to R1) due to the concomitant void fraction reduction and increased resistance to flow.

The TPR profile of the slurried catalysts is shown in Fig. 4. Four reduction areas can be observed: the first at 175–250 °C is ascribed to the decomposition of remaining nitrates; the second at 250–350 °C usually corresponds to the reduction of Co_3O_4 to CoO; the third at 350–600 °C is related to the reduction of CoO to metallic cobalt (Co^0); the last one at 800–1000 °C suggests de presence of cobalt aluminates which are difficult to reduce [35].

A representative XRD pattern of the calcined slurried catalyst is shown in Fig. 5, with the observed peaks matching those of cubic Co_3O_4 (JCPDS No. 00–001-1152) and Al_2O_3 (JCPDS No. 00–004-0875). The average crystallite size of Co_3O_4 particles was determined by applying the Scherrer equation to the most intense diffraction peak (36.8°). Subsequently, this value was adjusted using a correction factor of 0.75 to obtain the average diameter of metallic Co particles ($D_p(Co^0)XRD = 13$ nm), accounting for the molar volume reduction upon the conversion of Co_3O_4 to Co^0 [36].

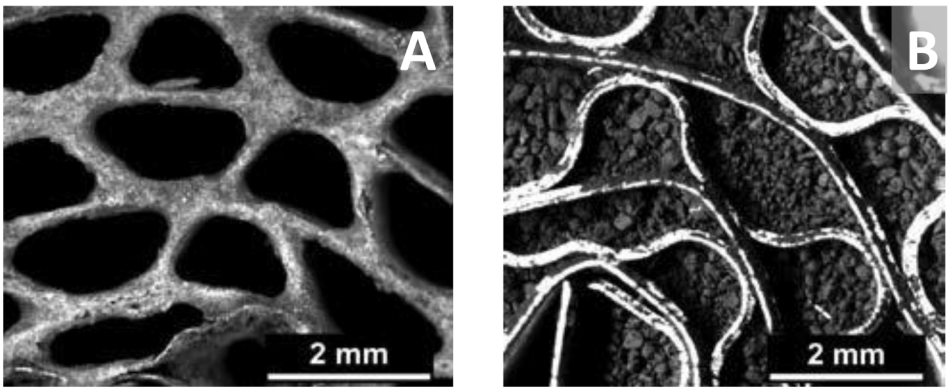

Fig. 2. Images of washcoated (A) and packed-bed (B) monoliths.

Table 2
Summary of the monolithic catalysts prepared.

Monolith type	Preparation method	Number of coatings	Catalyst volumetric hold-up (g_{cat}/cm^3)	δ (μm)[1]	$D_{Particle}$(μm)	L_D(μm)
R1_W36	Washcoating	25	0.33	36	–	36
R2_W40	Washcoating	36	0.33	40	–	40
R3_W62	Washcoating	41	0.33	62	–	62
R4_W83	Washcoating	48	0.33	83	–	83
R4_P150	Packing	–	0.82	–	150	25
R4_P250	Packing	–	0.78	–	250	42
R4_P400	Packing	–	0.74	–	400	67
R4_P650	Packing	–	0.49	–	650	108
R4_P950	Packing	–	0.41	–	900	150

[1] The average catalyst layer thickness (δ) was estimated using the expression $\delta = w_{cat.} \cdot \rho_{cat.}^{-1} \cdot S_g^{-1}$, where $w_{cat.}$ is the amount of deposited catalyst, ρ_{cat} is the average catalyst coating density (1.47 g/cm^3), the same that for the slurried catalyst particles, and Sg is the geometric surface area of the monolith (Table 1).

Table 3
Physicochemical properties of the structured catalysts.

Catalyst	N_2 physisorption			CO chemisorption
	S_{BET} (m^2/g)	V_{pore} (cm^3/g)	D_p (nm)	Co dispersion (%)
R1_W36	183	0.29	6.0	7.69
R2_W40	185	0.24	5.3	7.60
R3_W62	167	0.24	5.5	7.33
R4_W83	165	0.24	5.5	7.45
R4_P150	170	0.25	5.3	7.45
R4_P250	177	0.26	5.2	7.43
R4_P400	176	0.25	5.2	7.45
R4_P650	175	0.26	5.3	7.53
R4_P950	183	0.27	5.3	7.45

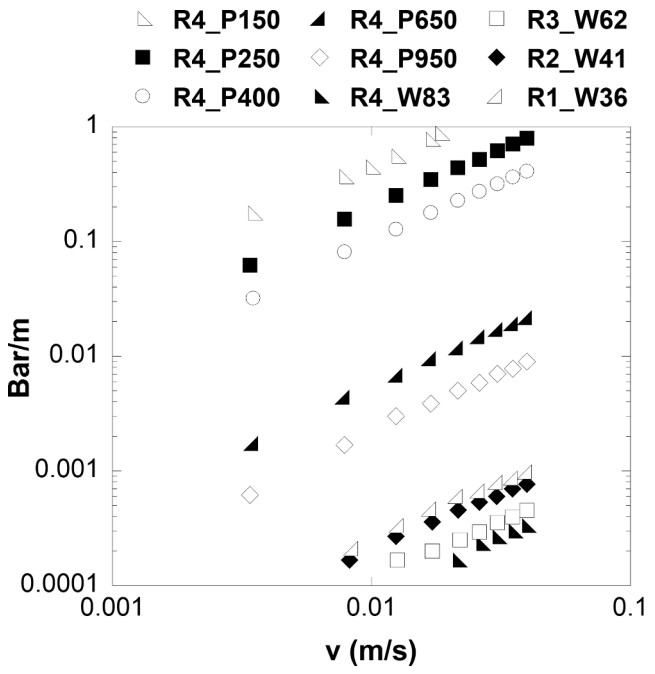

Fig. 3. Pressure drop of several washcoated and packed-bed monoliths.

3.3. Low-temperature FTS results

3.3.1. Washcoated monoliths: Effects of the cell density

Selectivity of the FTS is strongly influenced by the concurrence of transport limitations. In the case of the washcoated monoliths, transport limitations are mainly associated to the catalyst layer deposited onto the channels walls. The thickness of this layer (δ) will obviously depend on the geometric wall surface area available and the catalyst load, as evidenced by the results compiled in (Table 2). Therefore, it is important to analyze the performance of these reactors considering the average thickness of the corresponding catalyst layer.

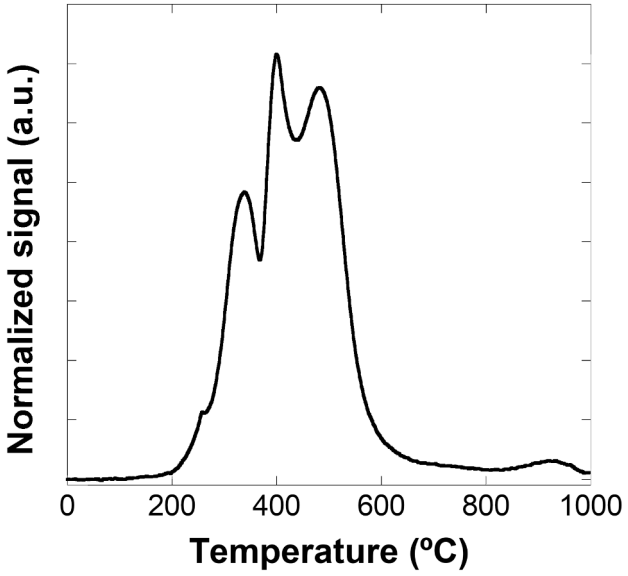

Fig. 4. TPR profile of slurried catalyst.

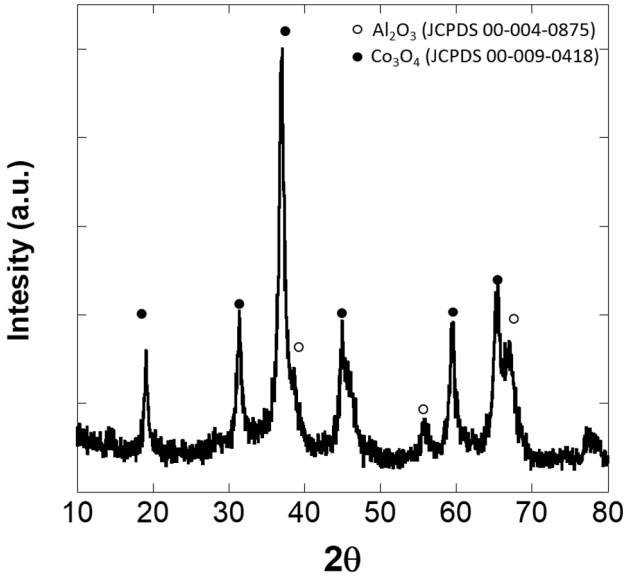

Fig. 5. XRD pattern of the slurried 20% Co – 0.5% Re/Al_2O_3 catalyst used.

CO conversion and selectivities to methane and C5+ yielded at steady state by the washcoated reactors are shown in Fig. 6. It can be

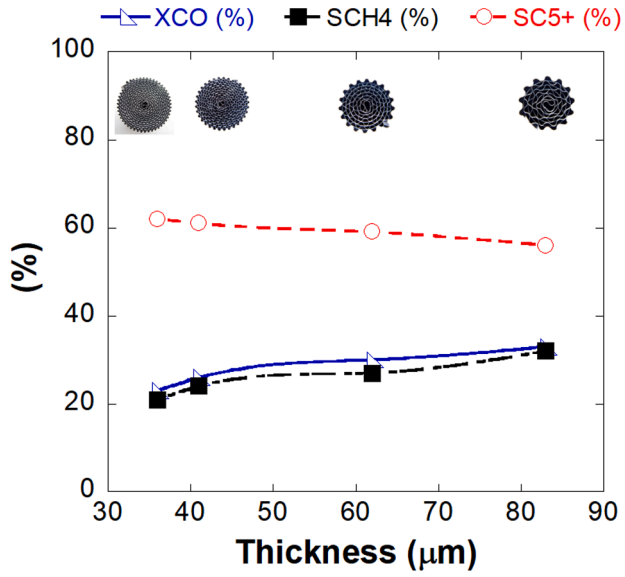

Fig. 6. Effect of the catalyst layer thickness on the CO conversion and selectivities to CH_4 and C5+ at steady state for washcoated monoliths R1_W36, R1_W40, R1_W62 and R1_W83. FTS conditions: 20 bar-a, 220 °C, syngas space velocity of 3 LN $g_{cat.}^{-1}\cdot h^{-1}$, and feed H_2/CO molar ratio of 2. Lines connecting experimental data dots are depicted for visual aiding purposes.

observed that both CO conversion and methane selectivity increase from around 20% for R1_W36 to slightly above 30% for R1_W83, *i.e.*, these magnitudes increase as the catalytic layer becomes thicker. Simultaneously, the selectivity values to C5+ decrease, thus indicating that the observed increased CO conversion is due to improved methane formation. It is well known that diffusional limitations within the catalyst layer increase the H_2/CO molar ratio due to the marked difference of diffusivity between the two components of syngas [37]. Therefore, the results shown in Fig. 6 are compatible with the increased influence of the mass transport limitations within the catalytic layer as its thickness increases.

In addition to the mass transport, heat transport properties have to be taken into account as well. The structure of the monolith is a very important factor in this regard. The effective radial thermal conductivity ($k_{e,r}$) of the raw aluminum monoliths used in this work are given in Table 1. It can be seen that $k_{e,r}$ decreases from 34.3 W/(m·K) for monolith R1 to 12.9 W/(m·K) for monolith R4. This is due to the higher void fraction associated to the decrease of the cell density that takes place from R1 to R4.

The radial (ΔT_R) and axial (ΔT_A) temperature differences within the structured reactors during the FTS experiments have been included in Table 4. The first one is the difference between the readings of the thermocouple located at the monolith center and that on the outer edge of the monolith at the same reactor length. The axial temperature difference (ΔT_A) is measured between the reaction temperature control point (220 °C), located at the exit of the monolith at r = 0, and the measurement point located at the monolith center. It can be seen that the temperature differences are very low; almost inexistent in the axial direction and only within 2–4 °C radially. In spite of the low differences, measurements are sensitive enough as to show that ΔT_R increases from R1 to R4, in accordance with the decrease of the effective radial thermal conductivity of the corresponding reactors. In spite of the low temperature differences found, these values may be sufficient to affect the catalytic activity. In a previous work by our groups, a simplified kinetic model was developed for the slurried catalyst used in the present study [38]. The apparent activation energies found for the methane and C5+ formation reactions were 110.2 kJ/mol and 62.6 kJ/mol, respectively. As the temperature control is performed with the central thermocouple, and axial temperature gradients are almost inexistent, a temperature of 220 °C can be assumed at the monoliths axis. At the monoliths outer edge the temperature at L/2 is between 2 °C (reactors R1_W36 and R2_W40) and 4 °C lower (reactor R4_W83) than in the monolith center. This allows to estimate a reduction of the CH_4 formation reaction between 9% and 25% at the outer edge compared to the monolith axis, whereas for the C5+ reaction, the rate decrease is limited to 6.5%-12% due to its lower apparent activation energy. The obvious conclusion is that the selectivity to C5+ will increase under the influence of radial heat transport limitations. As shown in Fig. 6, this is not the case; therefore, significant thermal effects on the FTS results of the monolithic washcoated reactors can be reasonably discarded, so that they can be considered isothermal under the experimental conditions of the present work.

3.3.2. *Packed-bed monoliths: Effect of the catalyst particle size*

The effect of catalyst particle size on the performance of conventional (unstructured) packed-bed reactors for the FTS was analyzed (Fig. 7A) and compared to that of the monolithic packed-bed reactors (Fig. 7B) under the same reaction conditions (3 LN $g_{cat.}^{-1}\cdot h^{-1}$, and feed

Table 4
Radial (R) and axial (A) temperature differences and hydrocarbons (C5+) productivity for structured monolithic reactors and conventional packed bed reactor during FTS experiments.

Reactor		ΔT_R (°C)	ΔT_A (°C)	Volumetric productivity(kg_{C5+}/ $m^3\cdot h$)	Per catalyst mass productivity(kg_{C5+}/ $kg_{cat.}\cdot h$)
Washcoated structured reactor	R1_W36	−2	−1	21.9	0.228
	R2_W40	−2	−1	24.3	0.254
	R3_W62	−3	0	27.1	0.283
	R4_W83	−4	0	28.3	0.296
Packed-bed structured reactor	R4_P150	−2	−1	21.5	0.090
	R4_P250	−2	−1	23.3	0.103
	R4_P400	−3	0	23.7	0.108
	R4_P650	−3	0	18.2	0.128
	R4_P950	−2	−1	20.4	0.171
Conventional packed bed reactor	$D_{particle}$= 150 μm V_{bed}= 2.93 cm^3	–	–	25.8	0.168
	$D_{particle}$= 250 μm V_{bed}= 3.08 cm^3	–	–	23.7	0.162
	$D_{particle}$= 400 μm V_{bed}= 3.25 cm^3	–	–	20.7	0.149
	$D_{particle}$= 650 μm V_{bed}= 4.90 cm^3	–	–	12.5	0.136
	$D_{particle}$= 950 μm V_{bed}= 5.86 cm^3	–	–	7.82	0.102

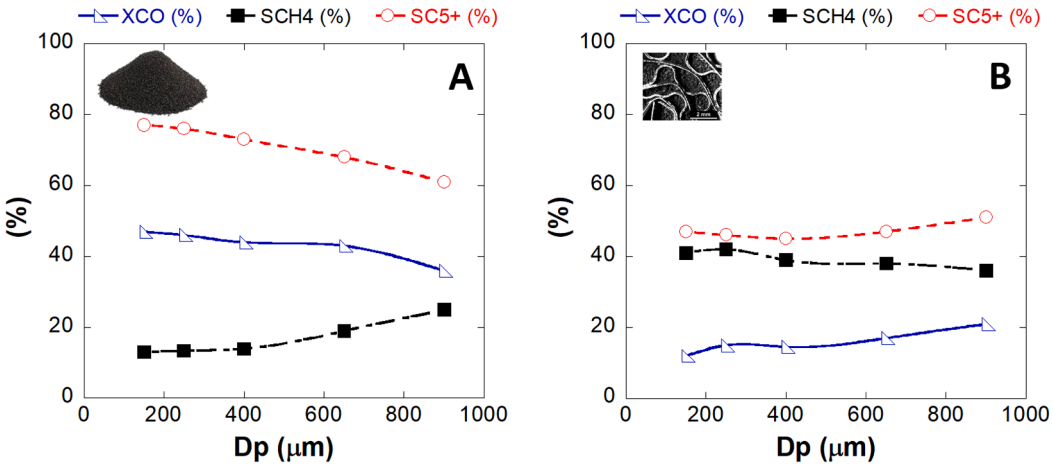

Fig. 7. Effect of the catalyst particle size on the CO conversion and selectivities to CH_4 and C5+ for the FTS in conventional packed-bed (A) and monolithic packed-bed (B) reactors. Lines connecting experimental data dots are depicted for visual aiding purposes.

H_2/CO molar ratio of 2). The slurried Co-Re/Al_2O_3 catalyst was diluted with silicon carbide particles to improve heat dissipation (450 mg of catalyst mixed with 2.25 g of SiC). It should be noted that in the monolithic packed-beds the catalyst was not diluted with SiC. In addition, the same R4 monolith was used to manufacture all the packed-bed structured reactors. It can be observed that the CO conversion achieved is higher in the conventional packed-bed reactors than in the structured ones. Whilst in the conventional packed-beds the CO conversion is around 40%, though it decreases slightly with the catalyst particle size, in the monolithic packed-beds, it is within 10%-20%, increasing slightly as the catalyst particle size increases. As for products selectivities, they also follow opposite trends. High C5+ selectivities are obtained in the conventional packed-beds, close to 80% in the case of the particles with mean size of 150 μm, diminishing to about 60% for the biggest particles of 950 μm. In contrast, C5+ selectivities remained relatively constant in the structured packed-beds, though increasing from 45% for R4_P150 to about 50% for R4_P950. Considering these results, methane selectivities were much higher in the structured packed-beds than in the conventional ones, as evidenced by the data presented in Fig. 7. Significant thermal effects can be also neglected in this case. Indeed, it is shown in Table 4 that axial temperature gradients are almost inexistent in the packed-bed monoliths, whereas radial gradients are somewhat less pronounced than for the washcoated monoliths, as expected from the improvement of the effective radial thermal conductivity resulting upon filling the void space of the microchannels with catalyst particles. In the case of the conventional packed-beds, dilution with SiC should additionally improve the heat transport properties.

3.3.3. C5+ hydrocarbons productivity

One of the main reasons behind the use of structured reactors is process intensification. Although this concept holds very diverse aspects, one of the most important, as concerns the FTS, is the productivity of C5+, which implies maximizing the catalyst hold-up and effectiveness. Volumetric and per catalyst mass C5+ productivities are presented in Table 4. Volumetric hydrocarbon productivity was referred to the total monoliths volume that showed an average value of 6.03 cm^3 or the total volume of the conventional packed-beds (catalyst particles mixed with SiC particles), and using an average C5+ hydrocarbons fraction density of 0.9 g/cm^3. As for the productivities obtained with the packed-bed monoliths, it can be seen that they vary from 18.2 $kg_{C5+}/(m^3 \cdot h)$ to 23.7 $kg_{C5+}/(m^3 \cdot h)$ without showing any clear trend regarding the catalyst particle size. However, when referred to the catalyst mass, 0.128 $kg_{C5+}/(kg_{cat.} \cdot h)$ and 0.171 $kg_{C5+}/(kg_{cat.} \cdot h)$ for R4_P650 and R4_P950 are obtained, respectively, compared to 0.090 $kg_{C5+}/(kg_{cat.} \cdot h)$ for R4_P150. It should be noted that, for a given monolith volume, the catalyst load decreases as the particle size increases. In this case, the loading is reduced by a factor of 2, from 0.82 $g_{cat.}/cm^3$ for R4_P150 to 0.41 $g_{cat.}/cm^3$ for R4_P950 (see Table 2). These results indicate that, within the range of particle diameters considered in this study, the monolithic packed-bed reactor performance for the FTS is significantly improved when catalyst particles of larger size are used. However, the behavior of the conventional packed-bed reactors followed the opposite trend as concerns the catalyst particle size (Table 2). In this case, the productivity per catalyst mass decreased from 0.168 to 0.102 $kg_{C5+}/(kg_{cat.} \cdot h)$ when increasing the catalyst particles diameter from 150 to 950 μm. Furthermore, as the particle size increases, the volume occupied by the bed, made up of both the catalyst particles and SiC particles, increases as well. This causes the volumetric productivity to decrease more markedly than the per catalyst mass productivity as the catalyst particle diameter increases. It is also noticeable that conventional packed-beds of particles of up to 650 μm in diameter give per catalyst mass productivities higher than those of the monolithic packed-beds containing particles of the same diameter. However, for the largest particles (950 μm), the per catalyst mass productivity of the structured

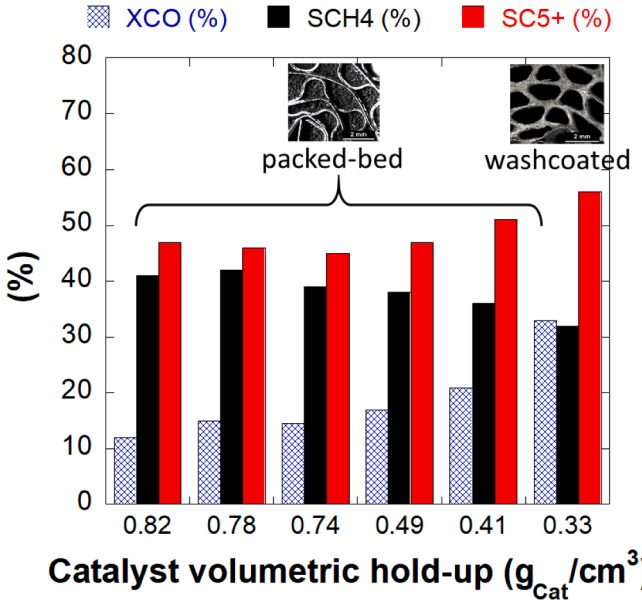

Fig. 8. CO conversion and selectivities to CH_4 and C5+ versus the catalytic load of the structured reactors manufactured using monolith R4.

packed-bed (0.171 $kg_{C5+}/(kg_{cat.}\cdot h)$) is much higher than that of the conventional packed-bed (0.102 $kg_{C5+}/(kg_{cat.}\cdot h)$).

Regarding the washcoated monoliths, the C5+ productivity is in general higher than for the packed-bed ones, increasing from 21.9 $kg_{C5+}/(m^3\cdot h)$ for R1_W36 to 28.3 $kg_{C5+}/(m^3\cdot h)$ for R4_W83. However, what is remarkable is that, due to their low catalyst loading (0.33 $g_{cat.}/cm^3$), the per catalyst mass productivities reach significantly high values within the 0.228–0.296 $kg_{C5+}/(kg_{cat.}\cdot h)$ range, almost doubling the productivity of the packed-bed monoliths. This means that washcoated monoliths are excellent contactors for the low-temperature FTS.

In order to further, compare the catalytic behavior of the structured monolithic reactors, Fig. 8 shows the CO conversion and CH_4 and C5+ selectivities obtained with all the reactors that share the same monolithic structure (R4). These reactors differ in the catalyst load (g_{cat}/cm^3) and the structuring method, packing or washcoating. It can be seen how the CO conversion increases for the packed-bed monoliths as the catalyst loading decreases due to the use of larger catalyst particles. The increased conversion, together with a relatively constant C5+ selectivity, lead to the increase of the hydrocarbons productivity described before for the packed-bed series of reactors. When the catalyst is incorporated by washcoating, the increase of both CO conversion and C5+ selectivity is remarkable, leading to the outstanding performance achieved by reactor R4_W83 in spite of its comparatively low catalyst content.

4. Discussion

In order to intensify the FTS in monolithic reactors, the catalyst hold-up needs to be optimized, achieving, in principle, the highest values possible that maximize the reactor volumetric productivity of the desired products while maintaining sufficiently low pressure drops.

Packed-bed monoliths are characterized by much higher catalyst hold-ups than their washcoated counterparts. The highest hold-up corresponds to the R4_P150 (0.82 $g_{cat.}/cm^3$) packed-bed monolith, whereas the lowest one (0.33 $g_{cat.}/cm^3$) is shared by the whole series of washcoated monoliths (Table 2). Higher hold-ups in packed-beds are obviously penalized with higher pressure drops across the reactor. In this regard, the highest pressure drop also corresponds to reactor R4_P150, but their range of values (0.2–0.8 bar/m) remains acceptable (Fig. 3). Ambrosetti *et al.* [39] found numerically and experimentally that pressure drops in packed-bed structured reactors are comparable or even lower than those observed in conventional packed-beds, for a given catalyst particle diameter. According to Schnitzelin [40] the packing structure causes local velocity fluctuations, which influence fluid-mechanical dispersion effects in the bed such as branching, and channeling due to the irregularities in the packing and the reactor walls. As a result, the porosity and the related pressure drop of packed beds is affected by their local structure. In catalytic wall reactors, pressure drop is much lower because the catalyst is in the form of a layer deposited onto the inner walls thus allowing unrestricted fluid flow across the center of the substrate channels [29,39]. Pressure drop is crucial for the potential use of monolithic catalyst in industrial applications, where it is important to reduce the compression costs and satisfy other constraints [41]. It should be noted that high pressure drops make the reactor less flexible to be scaled-up [19].

Analyzing the results provided by the packed-bed monoliths, it is observed that by increasing the size of the catalyst particles and, therefore, reducing the catalyst inventory, higher conversions of CO are obtained, while the selectivity to CH_4 decreases (Fig. 7B). As indicated in the previous section, significant heat transfer effects can be discarded as the cause for this result (Table 4). This behavior is opposite to that of a conventional fixed-bed (Fig. 7A), for which the CO conversion decreases and the methane selectivity increases significantly with increasing catalyst particle size. This feature of conventional fixed-beds is usually attributed to internal mass transport limitations through the waxes that fill the pores of the catalyst in the low-temperature FTS, leading to higher H_2/CO molar ratios than in the syngas feed [42]. However, it should be noted that two types of diffusional limitations occur in the low-temperature FTS: the slow removal of reactive products from pellets and reactors (the extra-pellet diffusion), and the slow arrival of reactants to the catalyst surface (the intra-pellet diffusion) [37]. The effect of the catalyst particle size on these phenomena is antagonist. On the one hand, as the particle size decreases, the number of inter-particle contact points increases producing waxes accumulation. On the other hand, as the particle size increases, the lower diffusivity of CO reduces the CO conversion and increases the H_2/CO ratio, thus increasing the methane selectivity. In our case, the effects of the extra-pellet diffusion in the conventional packed-bed seem to be of little importance within the range of particle sizes considered, possibly aided by the fact that the catalyst particles were highly diluted with SiC. That dilution generates voids that help to evacuate the heavier liquid products as they are formed.

This might be also a possible reason for the improved performance in terms of per catalyst mass productivity of the conventional packed beds compared to the structured ones observed for the smallest catalyst particles sizes (Table 4). As pointed out by Moulijn et al. the particle size has a tremendous effect on the hydrodynamics of multiphase flow in micro-packed-beds [43]. These authors found that radial mass transport could be an issue in the small reactors used for catalyst testing when conducting gas–liquid reactions. Differences can be even found between the so-called milli-reactors (reactor internal diameter of about 10 mm) and micro-reactors (reactor internal diameter of about 2 mm) [43]. Interestingly, in our case, the conventional fixed-bed reactors are closer to the milli-reactors, while the monolith channels filled with catalyst particles are closer to the micro-reactors, which further complicates the comparison of their performance. It should be also noted that in the FTS, the liquid phase is a reaction product that arises from the catalyst particles. Therefore, the situation is different to that of gas–liquid reactions where both the gas and liquid streams are fed to the reactor. As a result, the liquid hold-up should be high and essentially static, whereas the gas hold up should have an important dynamic component. It might be expected that this feature is more pronounced in the case of the monolithic packed-beds due to the small hydraulic diameter of the channels compared to that of the conventional packed beds. Therefore, perhaps the evacuation of the liquid hydrocarbons is difficult in the case of monoliths filled will the smallest particles, which would negatively affect the extra-pellet diffusion and the reactor performance.

As for the whascoated monoliths, both the CO conversion and methane selectivity increase, though slightly, as the cell density decreases and the catalytic layer becomes thicker (Fig. 6). The diffusion length, which directly corresponds to its thickness for a flat catalyst layer, is known to influence the FTS selectivity [9,14,23]. In this case, diffusional restrictions of reactants produce the expected methane selectivity increase, but accompanied by a rather surprising improvement of the CO conversion. Like for the packed-bed monoliths, significant heat transfer effects could be discarded as well. The radial temperature differences increase as the channel size and characteristic diffusion length increase, but the values achieved remain low as to evidence significant differences between the temperatures inside the various washcoated monoliths (Table 4).

Becker *et al.* [44] performed a simulation study on the effects of the catalyst layer thickness on the performance of washcoated monoliths operating under differential and integral conversion regimes and isothermal conditions. To understand the performance of these reactors it is very illustrative to consider the effect of the H_2/CO ratio on the different parameters describing the reaction. Under differential conversion conditions, the reaction rate increases with the H_2/CO ratio for a thin catalyst layer, as expected from the intrinsic (true) FTS kinetics [44]. In the case of a thick layer suffering from diffusional restrictions, the rate increases until reaching a H_2/CO ratio of about 1.8 and then only minor changes are observed, which is not strange due to stronger

diffusion limitations as the intrinsic kinetics becomes faster due to increased H_2 concentrations. However, for H_2/CO ratios between about 1.1 and 2, higher reaction rates are obtained with the thick layer compared to the thin one. This counterintuitive result comes just from the diffusional restrictions because, due to the different diffusivities of H_2 and CO, the H_2/CO ratio increases inside the catalyst layer with respect to the value in the fluid, overcompensating the effect of the lowered concentrations. The effect of the H_2 partial pressure on the kinetics is more important than that of CO due to the opposite effects of the concentration of CO that appear both in the numerator and as an adsorption term in the denominator of the Langmuir-Hinshelwood FTS rate equation.

As for the C5+ selectivity, a smooth s-shaped curve is obtained in the case of the thin layer, with near to 100% selectivity at very low H_2/CO ratios, a selectivity of about 80% at H_2/CO ratio of 2, and then, a continuous decrease of selectivity as the H_2/CO ratio further increases. In contrast, the curve is much more pronounced for the thick layer, resulting in a much lower C5+ selectivity of about 30% at H_2/CO ratio of 2 and further decreasing to only 10% at very high H_2/CO ratios. The different performance of the two layers is the expected one from the influence of the diffusional restrictions on the H_2/CO ratio in the case of the thick layer.

The fact that the H_2/CO ratio has opposite effects on the FTS rate and the C5+ selectivity leads to a maximum in the yield that is located above and below a H_2/CO ratio of 2 for the thin and the thick layers, respectively. Interestingly, the stoichiometry of the FTS causes that the ratio of the H_2 and CO consumptions is greater than 2 irrespective of the syngas H_2/CO ratio. This means that if syngas with a H_2/CO ratio of 2 is fed to the reactor, the fluid will contain the reactants with a sub-stoichiometric ratio (lower than 2) along the entire reactor. As thick layers exhibit maximum yields at H_2/CO ratios below 2, Becker *et al.* [44] state that these layers benefit from an operation under integral conditions (higher conversions).

The discussion above on the FTS kinetics allows explaining the increasing CO conversion values yielded by the washcoated monoliths, that follow the order R1_W36 < R2_W40 < R3_W62 < R4_W83 (Fig. 6). The resulting conversions do not deviate very much from the differential regime. Becker *et al.* found that diffusional limitations were relevant for catalyst layer thicknesses above 140 μm [44]. It is well known that the thickness establishing the transition to a diffusional-limited regime depends on the intrinsic activity of the catalyst and decreases as its activity increases. Becker *et al.* [44] used the kinetic model developed by Yates and Satterfield [45]. A higher activity can be expected for the more modern cobalt-based low-temperature FTS catalysts. In this regard, a catalyst with an activity factor 5 times higher than that of Yates and Satterfield leads to a layer thickness of about 80 μm as limiting value. Therefore, no (R1 and R2) or barely moderate (R3 and R4) diffusional restrictions can be expected for the washcoated monoliths investigated in this work. Due to the facts that the actual H_2/CO ratio is below 2 and that diffusional limitations increase this ratio, eventually overcompensating the lower H_2/CO ratio in the fluid bulk, it is possible that thicker layers (R3 and R4) suffering from diffusional restrictions give rise to moderately higher conversions than the thinner ones (R1 and R2) which operate at the actual H_2/CO ratio in the fluid bulk. Becker *et al.* [44] demonstrated that the presence of a liquid film containing the heavier FTS products does not introduce significant external transport limitations so the reactants concentrations on the external surface of the catalytic layer and in the fluid can be considered essentially the same.

In conclusion, within some limits, moderate mass transport limitations can be beneficial as concerns the FTS conversion due to the effects of the H_2/CO ratio on the reaction kinetics. Nevertheless, the selectivity to CH_4 increases moderately as the catalytic layer becomes thicker, evidencing the presence of diffusional restrictions that increase the H_2/CO ratio in the case of the monoliths R3 and R4. It is also important to note that the H_2/CO ratio of 2 typically used in research studies is not the optimal one, especially for thin catalytic layers.

Regarding the packed-bed monoliths, the CO conversions achieved follow a trend similar to that of the washcoated reactors, though they are lower and therefore closer to the differential regime. The mean diameters of the packed catalyst particles lead to equivalent diffusion lengths (L_D) within the 25 (R4_P150) – 150 μm range (R4_P950) and, as in the case of the washcoated monoliths, moderate diffusional restrictions can be expected only for the largest particles (Table 2). The increase of the CO conversion with the particle size (or L_D) can thus be explained as well by the effects of the H_2/CO ratio on the FTS kinetics, as pointed out by Vervloet *et al.* [38]. In this very important work, authors solved numerically the reaction–diffusion problem for the FTS in a spherical catalyst particle. The model developed was validated against experimental results from the literature. It is remarkable that this study has been the first one in which the variation of the local chain growth probability (α) is taken into account. A wide variety of catalyst particle radii, within 10^{-5}-10^{-3} m, and operating conditions (bulk H_2/CO ratio, temperature and pressure) were considered. The kinetics by Yates and Satterfield was adopted and it is nicely shown how CO is prone to suffer from strong mass transfer limitations resulting in an increased H_2/CO ratio towards the center of the catalyst particles. This negatively affected (lowering) the local chain growth probability, and then, the C5+ selectivity. As discussed by the authors, the gradients were due to intrinsically unbalanced diffusivities and consumption ratios of H_2 and CO [38]. This paper provides very useful practical guidelines for selecting the most favorable operating conditions in order to maximize the C5+ productivity. A very important finding is that the bulk H_2/CO ratio and the FTS temperature are strongly coupled. It is not possible to establish an optimum value for one of these magnitudes without specifying the other. In this regard, the C5+ productivity can be increased by a factor between 3 for small particles ($D_{Particle}$ = 50 μm) and 10 for large particles ($D_{Particle}$ = 2.0 mm) by lowering the H_2/CO ratio in the bulk gas phase from 2 to 1, and increasing the reaction temperature from 227 °C to 257 °C.

It should be noted that, as mentioned previously, the H_2 to CO Fischer-Tropsch consumption stoichiometry is greater than 2 in any case, and it is given by 3 – α, being α the chain growth probability [38]. In our case, α values increase in the following order: packed-bed monoliths (0.64–0.67) < washcoated monoliths (0.71–0.74) < conventional packed-beds (0.72–0.83). As a result, average consumption stoichiometries increase in the following order: conventional packed-beds (2.22) < washcoated monoliths (2.28) < packed-bed monoliths (2.34). Following Vervloet *et al.* [38], and taking into account the range of catalyst particle size or characteristic length used in our work, the reactor could be fed with syngas of H_2 to CO ratio of *ca.* 1.6–1.7 at 220 °C, and then, gradually increasing the reaction temperature along the reactor up to a maximum value of 240 °C. This would result in an average value of α with practical interest of 0.9.

CO conversions are significantly lower in the packed-bed monoliths compared to the washcoated reactors. Therefore, the H_2/CO ratios should be higher, though the consumption stoichiometry is slightly higher as well (2.34 vs. 2.28), thus explaining the higher selectivities to methane provided by the structured packed beds. Indeed, the washcoated monoliths provide CO conversions that are almost twice the values achieved in the packed-bed monoliths. For example, R3_W62 (L_D = 62 μm) gives a CO conversion of about 0.31 while the monolith R4_P400, loaded with particles 400 μm in diameter (L_D = 67 μm), yields a CO conversion of 0.14 (Figs. 6 and 7). When comparing these two structured reactors it should be noted that their hydrodynamic behavior is very different, as pointed out by Gascon *et al.* [24]. Low-temperature FTS is a gas–solid-liquid process. As the liquid phase is generated within the catalyst pores, a film flow can be initially established in washcoated monoliths that could evolve to a Taylor (segmented) flow favored by the small diameter of the channels and the moderate gas flow rate. This flow regime is characterized by a fast radial mass transport that will contribute to a good reactor performance. In contrast, (micro)packed-bed reactors show a specific behavior [24]. When the loaded particles

are small (typically below 200 μm in diameter), capillary forces predominate over the viscous and gravitational ones; this favors wetting of the particles by the liquid phase whereas the gas follows preferential paths and the reactor shows poor radial mass transport. When the ratio between the channel diameter and the catalyst particle size is low (between 1 and 2) a so-called single-pellet-string or composite structured packing reactor results [24]. This would be the case of R4_P650 ($D_H/D_{Particle} = 1.6$) and R4_P950 ($D_H/D_{Particle} = 1.2$) in this study. In the single-pellet-string reactor the flow regime is similar to that of empty tubes and mass transport is enhanced if a Taylor flow regime develops. This fact could contribute to obtain higher conversions as the particle size increases as experimentally observed with the packed-bed monoliths.

Comparing the performance of monolithic packed-bed reactors and conventional packed beds it has been found that, on average, the volumetric hydrocarbon production of the structured packed-bed reactors is higher than that of the conventional packed beds (Table 4). Vervloet *et al.* [29] demonstrated numerically that despite lower catalyst hold-up of structured packed bed reactors compared to the randomly packed bed, the structured ones could achieve 25% higher C5+ productivity per reactor volume than the conventional packed beds. This was attributed to the voids at internal walls of the structured substrate, and better removal of the increased amount of generated heat.

The preceding discussion has been performed considering the absence of thermal effects, *i.e.* isothermal conditions. The presence of internal and external heat transport limitations under conditions relevant to the low-temperature FTS are generally discarded [26,38]. However, the fact that internal and external heat transport limitations are absent does not allow discarding the presence of temperature gradients at the reactor (monolith) level. In this regard, the experimental measurements of the temperature along the axial and radial directions support the assumption of isothermal conditions (Table 4). Further support is given by the results of the calculations included in Appendix A.

It can expected that packed-bed monoliths have higher effective thermal conductivities than the washcoated ones, in accordance with the higher void fraction of the latter and the lower thermal conductivity of gases compared to solids [24]. Therefore, as concerns reactor isothermicity, the least favorable situation would correspond to the washcoated monoliths. An eventually higher mean temperature of the washcoated reactors compared to the packed-bed ones is compatible with higher CO conversions and methane selectivities, as experimentally observed (Table 4). However, it could hardly explain the increase of the conversion and methane selectivity with the thickness of the catalytic layer that is also found experimentally.

5. Conclusions

Structured monolithic reactors in which a state-of-the-art Co-Re catalyst is incorporated by washcoating outperform structured packed-bed monoliths containing the same (slurried and pelletized) catalyst in terms of both volumetric and per catalyst mass productivities of C5+, in spite of the lower catalyst hold-up of the former.

It has been found that, within the range of characteristic diffusion lengths or catalyst layer thicknesses considered in this work (36–83 μm), the CO conversion increases without significant loss of C5+ selectivity as the catalyst layer becomes thicker in the washcoated monoliths, giving rise to an increased hydrocarbons productivity. This behavior can be explained by the effects of mass transport limitations on the H_2/CO molar ratio, and that of this ratio on the FTS kinetics, resulting that the C5+ productivity during the low-temperature FTS benefits from moderate mass transport limitations. A positive effect of moderate mass transport limitations is also observed in the packed-bed monoliths. In this regard, slight increases of the CO conversion and the selectivity to C5+ take place in beds containing the biggest catalyst particles used (particle diameters of 650 and 950 μm, characteristic diffusion lengths of 108 and 150 μm, respectively).

To understand the highest performance (volumetric C5+ productivity) of the washcoated monoliths for the low-temperature FTS, the extra-pellet mass transport limitations that affect to the liquid hydrocarbons and waxes produced have to be taken into account. According to recent literature, the flow regime in the washcoated monoliths can evolve to one of the Taylor (segmented) type, characterized by very good radial transport properties and easier evacuation of liquids and waxes. This is not possible in structured packed-beds with small catalyst particles, in which the gas–liquid/solid contact is poor, resulting in a diminished effectiveness of the catalyst and a poorer reactor performance in spite of their comparatively higher catalyst hold-up. The hydrodynamic behavior of the monolithic packed-beds for the low-temperature FTS improves as the catalyst particle size increases, which may also contribute to the improved reactor performance observed.

Declaration of Competing Interest

The authors declare that they have no known competing financial interests or personal relationships that could have appeared to influence the work reported in this paper.

Acknowledgements

Financial support of this work was undertaken by the Basque Government (IT1069-16) and the Spanish Ministerio de Ciencia, Innovación y Universidades and the European Regional Development Fund (ERDF/FEDER) (grants RTI2018-096294-B-C31, RTI2018-096294-B-C32 and CTQ2015-73901-JIN). Open Access funding provided by University of Basque Country. Authors also acknowledge Micromeritics Instruments Corp. for the AutoChem II 2920 awarded and the technical and human support provided by SGIker of UPV/EHU (X-ray diffraction measurements). Luis M. Gandía wishes to thank Banco de Santander and Universidad Pública de Navarra for their financial support under the "Programa de Intensificación de la Investigación 2018" initiative.

Appendix A

A.1. Criterion for the absence of internal temperature gradients

The absence of internal temperature gradients inside the catalyst particles of a packed-bed monolith can be assumed if the following criterion is satisfied [38]:

$$\left(\frac{E_A}{R \cdot T}\right) \cdot \left(\frac{(-\Delta H_r) \cdot (-R)_{CO} \cdot \rho_{cat} \cdot l_{cat}^2}{\lambda_{cat} \cdot T}\right) < 0.05$$

E_A: apparent activation energy: 62,600 J/mol (C_{5+} formation); 110,200 J/mol ($C_{1\text{-}4}$ formation) [46].
R: 8.314 J/(mol·K)
T: 493 K.
$(-\Delta H_r)$: 165,000 J/mol.

ρ_{cat}, catalyst density: $1.47{\cdot}10^{6}$ g/m^3 [7].

λ_{cat}, catalyst thermal conductivity: 0.3 W/(m·K) [26].

$(-R)_{CO}$, reaction rate calculated under differential regime: $1.12–3.36{\cdot}10^{-5}$ mol(s·g_{cat}).

l_{cat}, characteristic dimension (least favorable conditions, *i.e.* thickest layer and largest particles): $8.3{\cdot}10^{-5}$ m (washcoated), $15{\cdot}10^{-5}$ m (packed-bed).

Under the worst conditions (highest reaction rate, formation of C_{1-4} only) the result is 0.010 for the wall coated monoliths and 0.033 for the packed-beds monoliths, so the criterion is safely fulfilled in both cases.

A.2. Criterion for the absence of external (interphase) temperature gradients

The presence of external interphase (gas–solid) heat transport limitations can be neglected if the fact the Mears' criterion is satisfied [26,38]:

$$\left(\frac{E_A \cdot (-\Delta H_r) \cdot (-R)_{CO} \cdot \rho_{cat} \cdot l_{cat}}{h \cdot R \cdot T^2}\right) < 0.05$$

h, film heat transfer coefficient: 5032 W/(m^2·K) [26].

Under the worst conditions (highest reaction rate, formation of C_{1-4} only) the result is 0.007 for the wall coated monoliths and 0.013 for the packed-bed monoliths so the criterion is safely fulfilled in both cases.

A.3. Criterion for the absence of radial temperature gradients at the reactor scale

Radial temperature gradients can be neglected in a catalytic bed if the Mears' criterion is satisfied [47]. Adopting the most restrictive case of significant heat transfer resistance at the reactor's walls, the criterion takes the form:

$$\left(\frac{|\Delta H_r| \cdot (-R)_b \cdot r_t^2}{k_e \cdot T_w}\right) < \frac{0.4 \cdot \frac{R \cdot T_w}{E_A}}{\left[1 + 8 \cdot \left(\frac{r_p}{r_t}\right) \cdot Bi_w\right]}$$

T_w: temperature at the reactor wall for which a value of 216 °C (489 K) is adopted for the worst case taking into account the radial temperature differences found (see Table 4).

r_t: reactor tube radius, $4{\cdot}10^{-3}$ m.

r_p: catalyst particle radius, $75{\cdot}10^{-6}$ m.

$|\Delta H_r|$: 165,000 J/mol.

$(-R)_b$: reaction rate per unit bed volume. Following Mears [47]:

$$(-R)_b = \frac{1-\varepsilon}{1+b} \cdot (-R)_{CO} \cdot \rho_{cat} = 2.6 - 5.3 \frac{mol}{s \cdot m^3_{bed}}$$

ε: bed void fraction (0.65–0.83). Estimated from the bed volumes (see Table 4) and composition (0.45 g of catalyst and 2.25 g of SiC). SiC density is $3.21{\cdot}10^{6}$ g/m^3 [48].

b : ratio of diluent to catalyst volume, 2.26.

k_e: effective thermal conductivity of the bed. According to Anderson et al. [49] this property has been volume averaged taking into account the bed porosity:

$$k_e = (1-\varepsilon) \cdot k_{solid} + \varepsilon \cdot k_{fluid}$$

Neglecting the fluid contribution and volume averaging the thermal conductivities of the catalyst (0.3 W/(m·K)) and the diluent (106.0 W/(m·K) [49]), k_{solid} = 73.6 W/(m·K) and k_e = 12.5–25.8 W/(m·K).

Bi_w: is the wall Biot number, for which values between 0.8 and 2 are typical [47].

Adopting the worst-case values of the several magnitudes, the criterion becomes:

$$0.0023 < 0.0113$$

It can be seen that the criterion is safely fulfilled for the conventional packed beds, which illustrates the positive effect of bed dilution. As for the structured reactors, the effective thermal conductivities of the substrates are within 12.9–34.4 W/(m·K) (see Table 1) which are higher than the value (12.5 W/(m·K)) used for the packed beds. The effective thermal conductivites of the washcoated, and especially the packed-bed, monolithic reactors should be higher than those of the substrates due to the presence of the catalyst. For these reasons, it is reasonable to expect that the left-hand term of the Mears criterion takes values lower than 0.0023 for the structured reactors thus allowing to discard the presence of significant radial temperature gradients in these systems.

References

[1] G. Chabot, R. Guilet, P. Cognet, C. Gourdon, A mathematical modeling of catalytic milli-fixed bed reactor for Fischer–Tropsch synthesis: Influence of tube diameter on Fischer Tropsch selectivity and thermal behavior, Chem. Eng. Sci. 127 (2015) 72–83, https://doi.org/10.1016/j.ces.2015.01.015.

[2] P. Piermartini, T. Boeltken, M. Selinsek, P. Pfeifer, Influence of channel geometry on Fischer-Tropsch synthesis in microstructured reactors, Chem. Eng. J. 313 (2017) 328–335, https://doi.org/10.1016/j.cej.2016.12.076.

[3] C. Zhu, G.M. Bollas, Gasoline selective Fischer-Tropsch synthesis in structured bifunctional catalysts, Appl. Catal. B 235 (2018) 92–102, https://doi.org/10.1016/j.apcatb.2018.04.063.

[4] S. Kook, L.M. Pickett, Soot Volume Fraction and Morphology of Conventional, Fischer-Tropsch, Coal-Derived, and Surrogate Fuel at Diesel Conditions, SAE Int. J. Fuels Lubr. 5 (2) (2012) 647–664, https://doi.org/10.4271/2012-01-0678.

[5] M.E. Dry, The Fischer–Tropsch process: 1950–2000, Catal. Today 71 (3-4) (2002) 227–241, https://doi.org/10.1016/S0920-5861(01)00453-9.

[6] C.G. Visconti, E. Tronconi, G. Groppi, L. Lietti, M. Iovane, S. Rossini, R. Zennaro, Monolithic catalysts with high thermal conductivity for the Fischer–Tropsch synthesis in tubular reactors, Chem. Eng. J. 171 (3) (2011) 1294–1307, https://doi.org/10.1016/j.cej.2011.05.014.

[7] A.Y. Khodakov, W. Chu, P. Fongarland, Advances in the Development of Novel Cobalt Fischer−Tropsch Catalysts for Synthesis of Long-Chain Hydrocarbons and Clean Fuels, Chem. Rev. 107 (5) (2007) 1692–1744, https://doi.org/10.1021/cr050972v.

[8] M.E. Dry, High quality diesel via the Fischer-Tropsch process - a review, J. Chem. Technol. Biotechnol. 77 (1) (2002) 43–50, https://doi.org/10.1002/jctb.527.

[9] D. Merino, O. Sanz, M. Montes, Effect of the thermal conductivity and catalyst layer thickness on the Fischer-Tropsch synthesis selectivity using structured catalysts, Chem. Eng. J. 327 (2017) 1033–1042, https://doi.org/10.1016/j.cej.2017.07.003.

[10] R.M. de Deugd, F. Kapteijn, J.A. Moulijn, Trends in Fischer–Tropsch Reactor Technology—Opportunities for Structured Reactors, Top. Catal. 26 (1-4) (2003) 29–39, https://doi.org/10.1023/B:TOCA.0000012985.60691.67.

[11] K. Pangarkar, T.J. Schildhauer, J.R. van Ommen, J. Nijenhuis, J.A. Moulijn, F. Kapteijn, Experimental and numerical comparison of structured packings with a

randomly packed bed reactor for Fischer–Tropsch synthesis, Catal. Today 147 (2009) S2–S9, https://doi.org/10.1016/j.cattod.2009.07.035.
[12] N. Hooshyar, D. Vervloet, F. Kapteijn, P.J. Hamersma, R.F. Mudde, J.R. van Ommen, Intensifying the Fischer–Tropsch Synthesis by reactor structuring – A model study, Chem. Eng. J. 207-208 (2012) 865–870, https://doi.org/10.1016/j.cej.2012.07.105.
[13] S. Saiedi, M.K. Nikoo, A. Mirvakili, S. Bahrani, N.A.S. Amin, M.R. Rahimpour, Recent advances in reactors fol low-temperature Fsicher-Tropsch synthesis: process intesification perspective, Rev. Chem. Eng. 31 (2015) 20–238, https://doi.org/10.1515/revce-2014-0042.
[14] L.C. Almeida, F.J. Echave, O. Sanz, M.A. Centeno, J.A. Odriozola, M. Montes, Washcoating of metallic monoliths and microchannel reactors, Stud. Surf. Sci. Catal. 175 (2010) 25–33, https://doi.org/10.1016/S0167-2991(10)75004-7.
[15] R. Guettel, J. Knochen, U. Kunz, M. Kassing, T. Turek, Preparation and Catalytic Evaluation of Cobalt-Based Monolithic and Powder Catalysts for Fischer−Tropsch Synthesis, Ind. Eng. Chem. Res. 47 (17) (2008) 6589–6597, https://doi.org/10.1021/ie800377n.
[16] R.M. de Deugd, F. Kapteijn, J.A. Moulijn, Using monolithic catalysts for highly selective Fischer–Tropsch synthesis, Catal. Today 79-80 (2003) 495–501, https://doi.org/10.1016/S0920-5861(03)00073-7.
[17] F. Kapteijn, R.M. de Deugd, J.A. Moulijn, Fischer–Tropsch synthesis using monolithic catalysts, Catal. Today 105 (3-4) (2005) 350–356, https://doi.org/10.1016/j.cattod.2005.06.063.
[18] A.-M. Hilmen, E. Bergene, O.A. Lindvåg, D. Schanke, S. Eri, A. Holmen, Fischer–Tropsch synthesis on monolithic catalysts of different materials, Catal. Today 69 (1-4) (2001) 227–232, https://doi.org/10.1016/S0920-5861(01)00373-X.
[19] C.G. Visconti, E. Tronconi, L. Lietti, G. Groppi, P. Forzatti, C. Cristiani, R. Zennaro, S. Rossini, An experimental investigation of Fischer–Tropsch synthesis over washcoated metallic structured supports, Appl. Catal. A 370 (1-2) (2009) 93–101, https://doi.org/10.1016/j.apcata.2009.09.023.
[20] O. Sanz, F.J. Echave, F. Romero-Sarria, J.A. Odriozola, M. Montes, in: Renewable Hydrogen Technologies, Elsevier, 2013, pp. 201–224, https://doi.org/10.1016/B978-0-444-56352-1.00009-X.
[21] T.A. Nijhuis, A.E.W. Beers, T. Vergunst, I. Hoek, F. Kapteijn, J.A. Moulijn, Preparation of monolithic catalysts, Catalysis Reviews 43 (4) (2001) 345–380, https://doi.org/10.1081/CR-120001807.
[22] F.J. Echave, O. Sanz, M. Montes, Washcoating of microchannel reactors with PdZnO catalyst for methanol steam reforming, Appl. Catal. A 474 (2014) 159–167, https://doi.org/10.1016/j.apcata.2013.07.058.
[23] A. Egaña, O. Sanz, D. Merino, X. Moriones, M. Montes, Fischer–Tropsch Synthesis Intensification in Foam Structures, Ind. Eng. Chem. Res. 57 (31) (2018) 10187–10197, https://doi.org/10.1021/acs.iecr.8b01492.s001.
[24] J. Gascon, J.R. van Ommen, J.A. Moulijn, F. Kapteijn, Structuring catalyst and reactor – an inviting avenue to process intensification, Catal. Sci. Technol. 5 (2) (2015) 807–817, https://doi.org/10.1039/C4CY01406E.
[25] B. Kaskes, D. Vervloet, F. Kapteijn, J.R. van Ommen, Numerical optimization of a structured tubular reactor Fischer-Tropsch synthesis, Chem. Eng. J. 283 (2016) 1465–1483, https://doi.org/10.1016/j.cej.2015.08.078.
[26] L. Fratalocchi, C.G. Visconti, G. Groppi, L. Lietti, E. Tronconi, Intensifying heat transfer in Fischer-Tropsch tubular reactors through the adoption of conductive packed foams, Chem. Eng. J. 349 (2018) 829–837, https://doi.org/10.1016/j.cej.2018.05.108.
[27] M. Iovane, R. Zennaro, P. Forzzati, G. Groppi, J.A. Lietti, E. Tronconi, C.G. Visconti, S. Rossini, E. Mignone, WO/2010/130399 (2010).
[28] F. Kapteijn, T.A. Nijhuis, J.J. Heiszwolf, J.A. Moulijn, New non-traditional multiphase catalytic reactors based on monolithic structures, Catal. Today 66 (2-4) (2001) 133–144, https://doi.org/10.1016/S0920-5861(00)00614-3.
[29] D. Vervloet, F. Kapteijn, J. Nijenhuis, J.R. van Ommen, Process intensification of tubular reactors: Considerations on catalyst hold-up of structured packings, Catal. Today 216 (2013) 111–116, https://doi.org/10.1016/j.cattod.2013.05.019.
[30] L. Fratalocchi, G. Groppi, C.G. Visconti, L. Lietti, E. Tronconi, Adoption of 3D printed highly conductive periodic open cellular structures as an effective solution to enhance the heat transfer performances of compact Fischer-Tropsch fixed-bed reactors, Chem. Eng. J. 386 (2020) 123988, https://doi.org/10.1016/j.cej.2019.123988.
[31] C.G. Visconti, G. Groppi, E. Tronconi, Accurate prediction of the effective radial conductivity of highly conductive honeycomb monoliths with square channels, Chem. Eng. J. 223 (2013) 224–230, https://doi.org/10.1016/j.cej.2013.02.095.
[32] S. Yasaki, Y. Yoshino, K. Ohkubo, US, 1993, pp. 5, 208, 206.
[33] L.C. Almeida, Sistemas de microcanales para la síntesis de Fischer-Tropsch, University of the Basque Country, San Sebastian, ES, 2010.
[34] O. Levenspiel, The Chemical Reactor Omnibook, OSU Book Stores, Corvallis (Oregon) 22.22, 1994.
[35] D. Merino, I. Pérez-Miqueo, O. Sanz, M. Montes, On the Way to a More Open Porous Network of a Co–Re/Al_2O_3 Catalyst for Fischer–Tropsch Synthesis: Pore Size and Particle Size Effects on Its Performance, Top. Catal. 59 (2-4) (2016) 207–218, https://doi.org/10.1007/s11244-015-0436-3.
[36] D. Schanke, S. Vada, E.A. Blekkan, A.M. Hilmen, A. Hoff, A. Holmen, Study of Pt-Promoted Cobalt CO Hydrogenation Catalysts, J. Catal. 156 (1) (1995) 85–95, https://doi.org/10.1006/jcat.1995.1234.
[37] E. Iglesia, S.C. Reyes, R.J. Madon, S.L. Soled, Selectivity Control and Catalyst Design in the Fischer-Tropsch Synthesis: Sites, Pellets, and Reactors, Adv. Catal. 39 (1993) 221–302, https://doi.org/10.1016/S0360-0564(08)60579-9.
[38] D. Vervloet, F. Kapteijn, J. Nijenhuis, J.R. van Ommen, Fischer–Tropsch reaction–diffusion in a cobalt catalyst particle: aspects of activity and selectivity for a variable chain growth probability, Catal. Sci. Technol. 2 (6) (2012) 1221, https://doi.org/10.1039/c2cy20060k.
[39] M. Ambrosetti, M. Bracconi, M. Maestri, G. Groppi, E. Tronconi, Packed foams for the intensification of catalytic processes: assessment of packing efficiency and pressure drop using a combined experimental and numerical approach, Chem. Eng. J. 382 (2020) 122801, https://doi.org/10.1016/j.cej.2019.122801.
[40] K. Schnitzlein, Modelling radial dispersion in terms of the local structure of packed beds, Chem. Eng. Sci. 56 (2) (2001) 579–585, https://doi.org/10.1016/S0009-2509(00)00263-3.
[41] G. Bellussi, M. Bohnet, J. Bus, K. Drautz, H. Greim, K.-P. Jackel, et al., Ullmann's Encyclopedia of Industrial Chemistry, seventh ed. (2011).
[42] M.F.M. Post, A.C. Van't Hoog, J.K. Minderhoud, S.T. Sie, Diffusion limitations in fischer-tropsch catalysts, AIChE J. 35 (7) (1989) 1107–1114, https://doi.org/10.1002/aic.690350706.
[43] J.A. Moulijn, M. Makkee, R.J. Berger, Catalyst testing in multiphase micro-packed-bed reactors; criterion for radial mass transport, Catal. Today 259 (2016) 354–359, https://doi.org/10.1016/j.cattod.2015.05.025.
[44] H. Becker, R. Güttel, T. Turek, Performance of diffusion-optimised Fischer–Tropsch catalyst layers in microchannel reactors at integral operation, Catal. Sci. Technol. 9 (9) (2019) 2180–2195, https://doi.org/10.1039/C9CY00457B.
[45] I.C. Yates, C.N. Satterfield, Intrinsic kinetics of the Fischer-Tropsch synthesis on a cobalt catalyst, Energy Fuels 5 (1) (1991) 168–173, https://doi.org/10.1021/ef00025a029.
[46] L.C. Almeida, O. Sanz, D. Merino, G. Arzamendi, L.M. Gandía, M. Montes, Kinetic analysis and microstructured reactors modeling for the Fischer–Tropsch synthesis over a Co–Re/Al2O3 catalyst, Catal. Today 215 (2013) 103–111, https://doi.org/10.1016/j.cattod.2013.04.021.
[47] D.E. Mears, Test for transport limitations in experimental catalytic reactor, Ind. Eng. Chem. Process Des. Develop. 10 (1971) 541–547, https://doi.org/10.1021/i260040a020.
[48] X. Zhu, X. Lu, X. Liu, D. Hildebrandt, D. Glasser, Heat transfer study with and without Fischer-Tropsch reaction in a fixed bed reactor with TiO_2, SiO_2, and SiC supported cobalt catalysts, Chem. Eng. J. 247 (2014) 75–84, https://doi.org/10.1016/j.cej.2014.02.089.
[49] R. Anderson, L. Bates, E. Johnson, J.F. Morris, Packed bed thermal energy storage: A simplified experimentally validated model, J. Storage Mater. 4 (2015) 14–23, https://doi.org/10.1016/j.est.2015.08.007.